

# Evaluating adsorption isotherm models for determining the partitioning of ammonium between soil and soil-pore water in environmental soil samples

Matthew G. Davis\*, Kevin Yan, Jennifer G. Murphy

5 Department of Chemistry, University of Toronto, Toronto, M5S 3H6, Canada

*Correspondence to:* Matthew G. Davis (mg.davis@mail.utoronto.ca)

**Abstract:** Ammonium in soil pore water is thought to participate in bidirectional exchange with the atmosphere; however, common soil nutrient analysis methods determine the bulk quantity of ammonium associated with the soil particles, rather than determining the aqueous ammonium concentration. Previous works have applied the Langmuir and Freundlich isotherm equations to ammonium-enriched soils to estimate partitioning, but this may not be representative of conditions in natural, unmanaged soils. In this work, environmental soil samples were collected from greenspaces in Toronto and used to evaluate several commonly used adsorption isotherm equations, including the Langmuir, Freundlich, Temkin and Toth equations, to determine their applicability in lightly managed and non-fertilized soils. We then compare ammonia emission potentials (a quantity predicting the propensity of ammonia to volatilize from a liquid reservoir) ~~determined~~<sup>calculated</sup> using a conventional ~~high-salt extraction procedure to determine the soil ammonium content~~<sup>nutrient-analysis method</sup> to that modelled using the Temkin and Langmuir equations, and demonstrate that conventional approaches may overestimate emission potentials from soils by a factor of 5 – ~~20~~<sup>2</sup>.

Key words: ammonium soil adsorption; emission potential;

## 1. Introduction:

### 20 1.1. Contextualizing the significance of ammonium partitioning in soils

Globally, emissions of reduced nitrogen compounds ( $\text{NH}_3$ ) make up as much as half of the global atmospheric reactive nitrogen sources (Flecharth et al., 2013). Of the  $\text{NH}_3$  budget, approximately two thirds of emissions are related to anthropogenic agricultural activities, with natural sources being responsible for only 15 – 20% of emissions (Bouwman et al., 1997; Sutton et al., 2008, 2013; Van Aardenne et al., 2001). Following emission,  $\text{NH}_3$  tends to partition into fine particulate matter or deposit via wet or dry deposition on a timescale of hours to days.  $\text{NH}_3$  is understood to engage in bidirectional exchange throughout the earth system, with  $\text{NH}_3$  depositing, or volatilizing depending on local environmental conditions (Farquhar et al., 1980; Flecharth et al., 1999, 2013; [Guo et al., 2022a](#); Nemitz et al., 2000; Sutton et al., 1995; [Walker et al., 2023](#); [Wentworth et al., 2014](#); [Zhang et al., 2010](#))). The bidirectional exchange of  $\text{NH}_3$  between soils and the atmosphere has been considered

important to its overall budget, particularly in remote areas, but research on the mechanics of  $\text{NH}_3$  partitioning in soils between adsorbed (inaccessible) and aqueous (accessible)  $\text{NH}_3$  often focuses on fertilized croplands with substantial concentrations of ammonia present (Venterea et al., 2015; Vogeler et al., 2011). ~~Consequently, ammonia volatilization models may parameterize all or most of the soil ammonia as being readily able to exchange with the atmosphere, which may be reasonable for recently fertilized soils, but not for unmanaged soils (Massad et al., 2010a; Pleim et al., 2013a; Zhu et al., 2015a).~~ However, cropland is estimated to make up less than 15% of the Earth's land area, while unfertilized or irregularly fertilized natural, semi-natural or pastoral land reflects nearly three quarters of terrestrial surfaces (Ellis et al., 2020). The short atmospheric lifetime of  $\text{NH}_3$  makes it important to understand the exchange of  $\text{NH}_3$  over all types of surfaces, despite agricultural cropland being the most globally significant source.

## 1.2. Importance of developing an ammonium adsorption partitioning model

Ammonium in soils is thought to be partitioned between  $\text{NH}_4^+$  (ads) adsorbed to soil particles and  $\text{NH}_4^+$  (aq) dissolved in soil pore water. Because soils tend to exist with both permanent and pH-dependent negative charges (Bache, 1976),  $\text{NH}_4^+$  ions compete for adsorption against other cations in solution. The total quantity of cations that can adsorb to the soil particles is termed the cation exchange capacity (CEC, typically reported as centimoles positive charge/kg). Traditional methods for determining ammonium in soil—intended for nutrient analysis in which the total ammonia nitrogen is more important than the partitioning between  $\text{NH}_4^+$  (ads) and  $\text{NH}_4^+$  (aq)—use high concentration salt solutions to displace all cations from the soil. As a result, these approaches do not distinguish between  $\text{NH}_4^+$  (aq) and  $\text{NH}_4^+$  (ads) (Li et al., 2012) and therefore likely overestimate the emission potential of soils. In this manuscript, we explore a variety of adsorption isotherm models with the goal of identifying a simple approach to relate the ~~total~~ quantity of ammonium in a soil ~~to the aqueous fraction of ammonium that can sample able to~~ participate in bidirectional exchange with the ~~atmosphere, total amount of ammonium, as a function of other readily measurable quantities.~~

## 1.3. Adsorption Isotherm equations:

The adsorption behavior of molecules to surfaces is complex and dependent on the properties of both the surface and the adsorbed molecules. Numerous adsorption equations have been proposed, based on both theoretical and empirical models; however, as the partitioning of ammonium between soil pore water and soil particles is complex and influenced by many other simultaneous equilibria, we consider each of the examined equations as being empirically determined only, rather than based on a theoretical treatment of the system. Previous studies have sought to develop an adsorption model for  $\text{NH}_4^+$  partitioning soils based on the Langmuir (Alnsour, 2020; Venterea et al., 2015) and Freundlich equations (Vogeler et al., 2011), but have focused on croplands and other agricultural soils. In this work, in addition to the Langmuir and Freundlich equations, we also investigate the application of the Temkin and Toth adsorption equations to  $\text{NH}_4^+$  partitioning in soils. Each of these equations (as formulated in ~~Table 1~~Table 1) represents the adsorbed  $\text{NH}_4^+$  concentration ( $S$ ,  $\text{mg kg}^{-1}$ ) in terms of the  $\text{NH}_4^+$  concentration in solution ( $C$ ,  $\text{mg L}^{-1}$ ). Except for the Freundlich equation, each of these equations incorporate a saturation point or maximum

adsorption capacity ( $S_{\max}$ , mg kg<sup>-1</sup>), ~~in which this work, we investigate -treats as an experimentally determined value equivalent to the potential to calculate these adsorption equations as a function of the measured CEC (-converted to mg of NH<sub>4</sub><sup>+</sup> kg<sup>-1</sup>soil), rather than treating  $S_{\max}$  as a calculated fitting parameter.~~

**Table 1:** Adsorption isotherm equations applied in this work and their parameters

Adsorption Isotherm Model	Equation	Units	Reference
Langmuir	(1) $S = \frac{S_{\max}k_L C}{1+k_L C}$	$S_{\max}$ (mg kg <sup>-1</sup> ), $K_L$ (L kg <sup>-1</sup> )	(Langmuir, 1916)
Freundlich	(2) $S = k_F C^{n_F}$	$k_F$ , $n_F$ (dimensionless)	(Freundlich, 1909)
Temkina	(3) $S = q_T \ln(1 + K_T C)$	$q_T$ (product of $S_{\max}$ (mg kg <sup>-1</sup> ) and $\frac{RT}{b}$ (dimensionless)), $K_T$ (L mg <sup>-1</sup> )	(Temkin & Pyzhev, 1940)
Toth	(4) $S = \frac{bc}{(K_{T0} + C^{n_T})^{\frac{1}{n_T}}}$	$b$ (product of $S_{\max}$ (mg kg <sup>-1</sup> ) and a dimensionless scaling factor), $K_{T0}$ (mg L <sup>-1</sup> ), $n_T$ (dimensionless)	(Tóth, 1995)

65 a The Temkin model is also given as  $S = \frac{RT}{b} \ln K_T C$ , see (Chu, 2021) for this formulation

## 2. Methods:

### 2.1. Soil Collection:

70 Soil samples were collected from several greenspace (parks, urban forest, roadside-sites, etc.) locations across Toronto. Samples were collected only on days preceded by at least two days without precipitation and were collected by inserting a 7.5 cm internal diameter steel tube into the ground to a depth of 5 – 10 cm and recovering a soil core by removing the tube from the ground. The soil cores were mixed, and sieved immediately, and transported back to the lab for analysis. Samples analyzed for NH<sub>3</sub> content were always analyzed immediately to avoid potential artefacts from freezing, samples analyzed for CEC or adsorption curves were frozen for storage prior to analysis. Soil samples were collected from eight locations in Fall 2021 as a training set for developing the model. A subsequent 16 soil samples from across Toronto were collected in Spring/Summer 75 2023 to be used to evaluate the effectiveness of applying the model to uncharacterized soils, and to determine the impact on soil emission potentials.

### 2.2. Soil analysis:

#### 2.2.1. Cation Exchange Capacity determination

80 The CEC was determined using the inductively-coupled plasma optical emission spectroscopy (ICP-OES) cation sum method (Bache, 1976). Briefly, 1 g of soil was measured out and mixed with 25 mL of 1 M NH<sub>4</sub>Cl, shaken, and refrigerated for 36 - 48 hours to settle. The supernatant was filtered using 0.2 um syringe filters, diluted 50-fold using volumetric glassware and analyzed for the common soil-associated cations, Na<sup>+</sup>, K<sup>+</sup>, Mg<sup>2+</sup>, and Ca<sup>2+</sup>. The ICP-OES was calibrated using a commercially available mixed standard of 6 cations (Li<sup>+</sup>, Na<sup>+</sup>, NH<sub>4</sub><sup>+</sup>, K<sup>+</sup>, Mg<sup>2+</sup>, Ca<sup>2+</sup>) (Thermo Fisher Scientific). Another soil-associated

cation that can contribute to CEC is  $Al^{3+}$ , our initial measurements screened for Al, but we did not detect it in solution. The  
85 CEC was determined for all 24 collected samples and used to select three of the soil samples from the 16 collected in 2023 to  
be used as a test set for the developed model.

### 2.2.2. Adsorption curve characterization

The determination of the adsorption behavior of  $NH_4^+$  was performed using a modified version of the procedurean approach  
similar to that described by Venterea et al. (2015), combined with the ICP-OES cation sum method (Bache, 1976). Briefly, a  
90 series of batch equilibrium samples were prepared by mixing 1 g of soil with 25 mL aliquots of  $NH_4Cl$  solutions with  
concentrations ranging from 2.5 – 1000 mM. The samples were shaken, refrigerated for 36 – 48 hours to settle, filtered with  
0.2  $\mu m$  syringe filters, diluted 50-fold with volumetric glassware, and analyzed using ICP-OES. The quantity of  $NH_4^+$  adsorbed  
onto each soil was ~~then~~ inferred based on the displaced  $Na^+$ ,  $Mg^{2+}$ ,  $Ca^{2+}$  and  $K^+$  ions measured in solution. In the cation sum  
method, the total quantity of adsorbable cations is determined by saturating the soil with an index cation (in this procedure,  
95 and generally,  $NH_4^+$  from  $NH_4Cl$ ), which displaces the original cations in the soil's adsorption sites. Thus the displaced cations  
measured for each  $NH_4Cl$  solution concentration are representative of the quantity of  $NH_4^+$  adsorbing onto the soil. Adsorption  
curves were determined for the original eight soil samples in the training set, as well as the three selected soil samples for the  
test set.

### 2.2.3. pH and $NH_4^+$ determination

100 pH and  $NH_4^+$  content was determined for the 16 soil samples collected in 2023. pH was determined for each soil sample using  
a typical approach of mixing soil with DIW in a 1:1 ratio, and then measuring the pH of the slurry by immersing a pH electrode  
(Hach) until a stable pH reading was obtained. To determine the pH using an alternative extraction solution, this process was  
repeated using a 0.01 M  $CaCl_2$  solution.

$NH_4^+$  was extracted from the soil using a batch equilibrium method using both a 2 M KCl extraction solution and a  
105 DIW solution. In both cases, 2.5 g of soil was mixed with 25 mL of the extraction solution, shaken, and refrigerated for 36  
hours to allow suspended solids to settle out of solution. Afterward, the supernatant was filtered using 0.2  $\mu m$  PES membrane  
syringe filters. The soil  $NH_4^+$  was quantified using the indophenol-blue salicylate method (Kempers & Zweers, 1986). Briefly,  
two reagent solutions, A and B were prepared: Reagent A consisted of a solution of 1 M sodium salicylate and 100  $mg L^{-1}$   
sodium nitroprusside, while Reagent B consisted of a solution of 1 M NaOH and 0.12% by volume of 5% available chloride  
110 NaOCl. Soil extracts were prepared for analysis by adding 0.6 mL of reagent A to 2 mL of soil extract, followed by the addition  
of 1.4 mL of reagent B. The mixtures were then stored for 2 hours in the dark for color development, and then quantified using  
UV-VIS spectrometry (Lambda 365, Perkin-Elmer) at 649 nm.

## 2.3. Data analysis:

### 2.3.1. Characterizing adsorption parameters using a training and test set

115 Curve-fitting was done in R using the nls function to fit our experimental data for the eight samples in our training set to the Langmuir, Freundlich, Temkin, and Toth equations. Goodness of fit was evaluated by calculating the Akaike information criterion ( $R^2$  is a poor criterion (AIC) using for non-linear models (Spiess & Neumeier, 2010), the residual standard error (RSE) was used to evaluate the AIC function from goodness of fit, where the R stats package. The AIC is calculated using equation (5):

$$(5) AIC = 2K - 2\ln(L)$$

120 Where  $K_{RSE}$  is the numbersquare-root of independent variables, and L is the log-likelihood estimate. The log-likelihood estimate can be extracted directly from nls objects fitted in R using sum of the AIC function, squared-residuals divided by the degrees of freedom, expressed as a percentage of the geometric mean response variable (Eq. (5)):

$$(5) RSE (\%) = \frac{\sqrt{\frac{1}{df} \sum (y - \hat{y})^2}}{\exp\left(\frac{1}{n} \sum \ln(y)\right)}$$

125 Fitting Average fitting parameters for each equation were determined in two ways: 1) by fitting each equation to the adsorption curve of each sample, and averaging the resulting fitting parameters, and 2) by pooling all the experimental data, standardizing each adsorption curve by the maximum adsorption achieved (i.e., all curves went from 0 to 1), and then fitting each equation from Table 1 to those curves.

To validate the effectiveness of these equations when applied to uncharacterized soil samples, we selected three soil samples from the 16 soil samples collected in 2023 to form a test set, these samples were selected by choosing the soil samples with the lowest (10.9) and highest CECs (37.2), and a soil with an average CEC (25.3). As the original training set mostly consisted of samples with CECs from 20 – 30 (with two samples with CECs of 7.6 and 16), we chose two samples that were significantly different than the average training set sample, as well as one similar sample to determine whether the fitting parameters could be used for 'extreme' samples, or only for samples similar to the training set. The test set was characterized in the same way as the training set, and was then modelled using three approaches:

- 135
- i. Using the average CEC for all the soil samples of 25 cmole kg<sup>-1</sup> ( $S_{max}$  of 4500 mg kg<sup>-1</sup>), and the training set parameters.
  - ii. Using the measured CEC for each soil sample to calculate  $S_{max}$ , and the training set parameters.
  - iii. Using the fitting algorithm as described in Sect.2.3.1 above to determine the least squares fit for each equation to the experimental data.

### 2.3.2. Emission potential determination

140 The emission potential of ammonia is a quantity calculated as the ratio of aqueous  $NH_4^+$  to  $H^+$  (Eq. (6)). (6).

$$(6) \Gamma = \frac{[NH_4^+]}{[H^+]}$$

Commonly, for soils this would be calculated using the total  $\text{NH}_4^+$  (determined using a salt solution extraction) and the pH measured using an extraction with deionized water. We denote this as  $\Gamma_{\text{STD}}$ , corresponding to  $\frac{[\text{NH}_4^+]_{\text{salt}}}{[\text{H}^+]_{\text{DIW}}}$ . The pH may also be measured in a (less concentrated) salt solution, which we denote as  $\Gamma_{\text{SALT}}$ , corresponding to  $\frac{[\text{NH}_4^+]_{\text{salt}}}{[\text{H}^+]_{\text{salt}}}$ . Similarly, though we are not aware of this as a common method,  $\text{NH}_4^+$  could be determined using a DIW extraction solution, resulting in a third parameterization of the emission potential as  $\Gamma_{\text{DIW}}$ , representing  $\frac{[\text{NH}_4^+]_{\text{DIW}}}{[\text{H}^+]_{\text{DIW}}}$ . Lastly, by applying one of the adsorption isotherm models, the total soil  $\text{NH}_4^+$  can be partitioned into  $\text{NH}_4^+_{(\text{ads})}$  (S) and  $\text{NH}_4^+_{(\text{aq})}$  (C), and the emission potential can be calculated using only the  $\text{NH}_4^+$  in solution (C). These versions of the emission potential are denoted as  $\Gamma$ -sub-equation-name (e.g., as  $\Gamma_{\text{Langmuir}}$ ,  $\Gamma_{\text{Temkin}}$  etc).

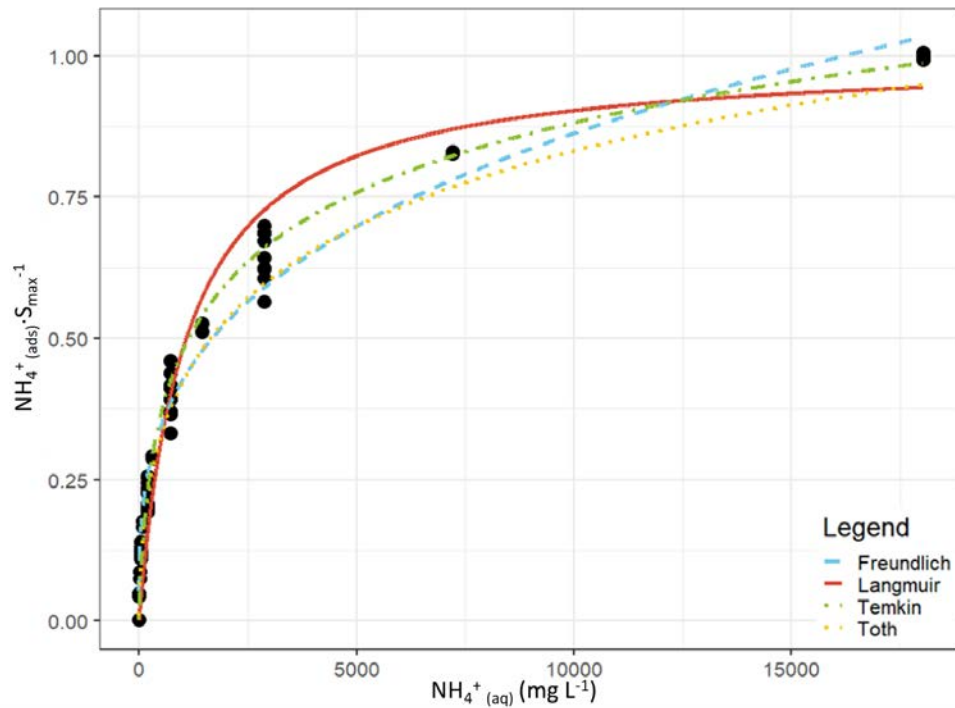
### 150 3. Results:

#### 3.1. Performance of adsorption isotherm equations applied to an environmental soil training and test set:

We evaluated the ability of the Langmuir, Freundlich, Temkin and Toth equations to model the partitioning of  $\text{NH}_4^+$  between adsorbed and aqueous forms. An We did this both by fitting the adsorption curve was characterized for each soil, separately, and by standardizing each adsorption curve to its maximum adsorption, and then pooling the data from each soil adsorption experiment was pooled, and then fit using the R nls function. The adsorption curves and fitting parameters are shown in Figure 1 and Table 2. Additionally, as our interest is ultimately in and fitting the performance of these adsorption equations at the lower concentration limit, we refit each equation using only the extraction solutions  $<680 \text{ mg L}^{-1} \text{ NH}_4\text{Cl}$  resulting data. The adsorption curves and fitting parameters under those conditions for the pooled data approach are shown in Fig. 1 and Table 2, the equivalents for the separate fit approach are shown in Figure 2 and Table 3. Fig. A1 and Table A1. The fitting parameters determined with these two approaches are approximately equivalent to one another and could be used interchangeably (with the exception of the Toth equation parameters, which will be discussed further below).

While the Langmuir (Alnsour, 2020; Guo et al., 2022b2022; Venterea et al., 2015) and Freundlich (Vogeler et al., 2011) equations have been previously reported as being effective at modelling  $\text{NH}_4^+$  partitioning in soils, we found them to be the least effective of the equations we examined for the full adsorption curves, both over- and under-estimating the adsorbed  $\text{NH}_4^+$  concentrations (Figure 1), while the (Fig. 1) with consistently high residuals (Table 2: 24% RSE (Langmuir), 15% RSE (Freundlich)). The Temkin and Toth equations better fit the experimental data. Computing the Akaike information criterion for these equations results in an AIC of -138, -190, -222, and -249 for the Langmuir, Freundlich, have smaller RSE's of 12% (Temkin,) and 9.0% (Toth equations respectively. The absolute value of the AIC is not important, but for a set of models, the model with the lowest AIC is considered the best at fitting the experimental data, indicating an order of). The Toth and Temkin > Freundlich > Langmuir for model effectiveness. However, fitting only the equations have even lower range of the adsorption curves (0 – 40 mM) slightly changed these results, the Toth equation could not be residuals for the individually fit

by our algorithm, and the resulting AIC values were -93, -157, -152 for the Langmuir, Freundlich, and curves (A1, A2), 3.0–16.1% (Temkin equations respectively, indicating that the Freundlich equation best fit the experimental data. (Note that AIC values for models fit to different datasets should not be directly compared to one another.)), and 0.9–6.5% (Toth).





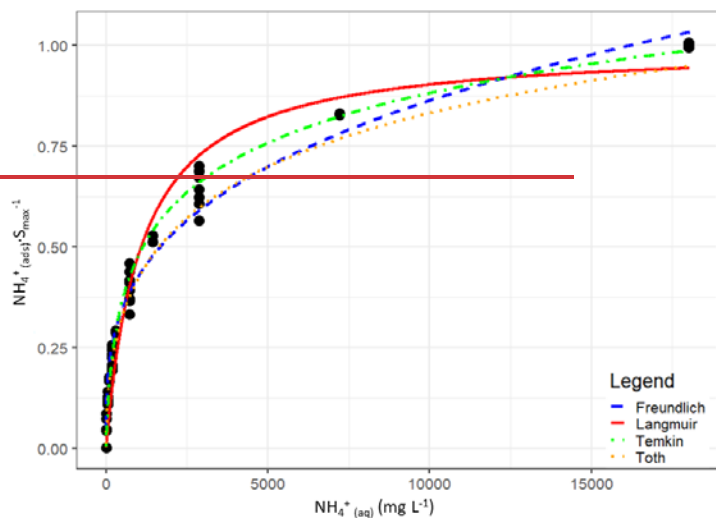


Figure 1: Curve-fitting comparison between the Langmuir (red, solid), Freundlich (blue, ---), Temkin (green, - · - ·), and Toth (orange, · · ·) equations. The curves are plotted using the experimental data from all eight soil adsorption experiments, standardizing the y-axis is normalized to by the maximum adsorption achieved during each experiment.

180

Table 2: Comparison of goodness of fit residual standard errors and fitting parameters for of the selected adsorption equations pooled fitting parameters

Equation	Number of fitted parameters	<u>AIC</u> <u>RSE</u>	Parameter 1	Mean ± Standard error	Parameter 2	Mean ± <u>Standard error</u> <u>RSE</u>	Exponential Factor
Langmuir	1	<u>-1382.4%</u>	$K_L$	$9.29 \cdot 10^{-4} \pm 5.9 \cdot 10^{-5}$	$S_{max}$	-	-
Freundlich	2	<u>-190.5%</u>	$K_F$	$S_{max} * 0.0520 \pm 3.4 \cdot 10^{-3}$	-	-	$0.3050 \pm 0.0074$
Temkin	2	<u>-222.2%</u>	$K_T$	$1.33 \cdot 10^{-2} \pm 1.2 \cdot 10^{-3}$	$q_T$	$S_{max} * 0.180 \pm 4.1 \cdot 10^{-3}$	-
Toth	3	<u>-2499.0%</u>	$K_{To}$	$3.10 \pm 0.65$	$b$	$S_{max} * 2.45 \pm 0.35$	$0.25 \pm 0.027$

Formatted Table

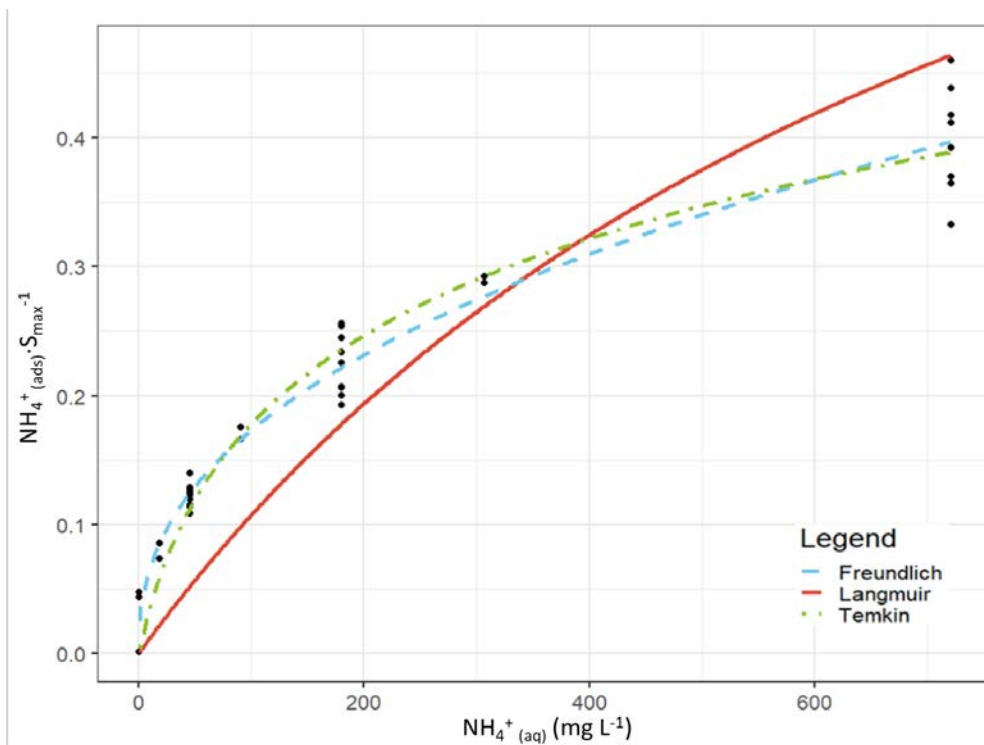


Figure 2: Curve-fitting comparison between the Langmuir (red, solid), Freundlich (blue, ---), and Temkin (green, - · -) equations. The curves are plotted using the experimental data from all eight soil adsorption experiments, but only using the extraction solutions of <40 mM for fitting, the y-axis is normalized to the maximum adsorption achieved during each experiment. The Toth equation could not be fit to the experimental data under these conditions.

Table 3: Comparison of goodness of fit and fitting parameters for the selected adsorption equations, data fit only for the <40 mM solutions

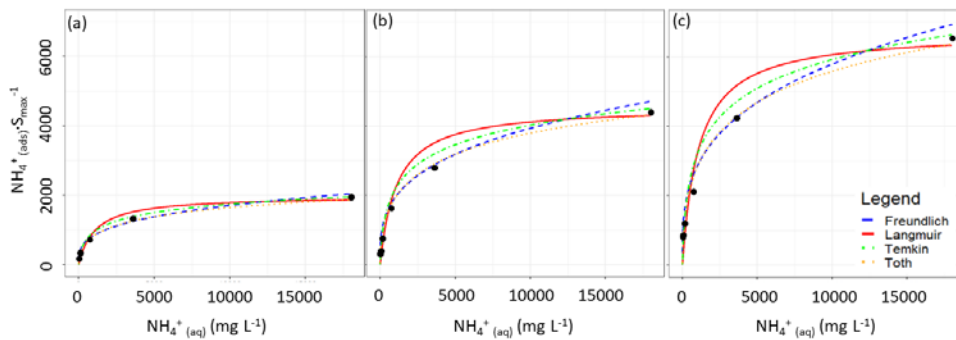
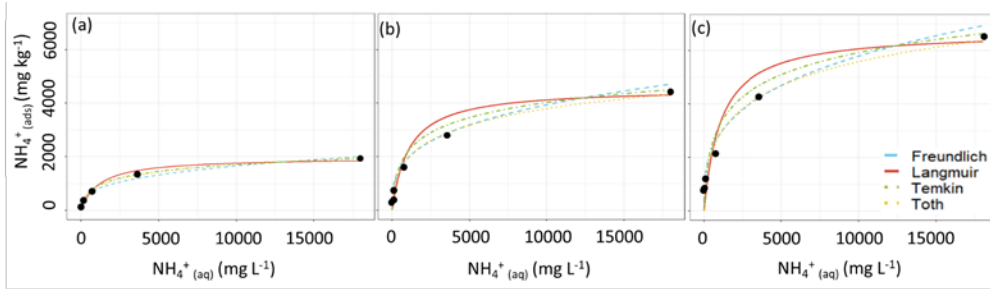
Equation	Number of fitted parameters	AIC	Parameter 1	Mean ± Standard error	Parameter 2	Mean ± Standard error	Exponential Factor
Langmuir	1	-93	$K_L$	$1.2 \cdot 10^{-3} \pm 8.0 \cdot 10^{-4}$	$S_{max}$	=	=
Freundlich	2	-157	$K_F$	$S_{max} * 0.025 \pm 3.0 \cdot 10^{-3}$	=	=	$0.42 \pm 0.019$

Temkin	2	-152	$K_T$	$\frac{3.4 \cdot 10^{-2} \pm 6.5 \cdot 10^{-3}}$	$q_T$	$\frac{S_{max} \cdot 0.120 \pm 8.5 \cdot 10^{-3}}$	=
Toth	3	Fit did not converge					

With our objective being to evaluate how well each equation can fit soils without going through the full characterization procedure, we analyzed the adsorption curves of the low-CEC, medium-CEC and high-CEC soils in our test set using: i) a “typical” CEC of 25, and the fitting parameters from [Table 2, Table 2](#), ii) the measured CEC and the fitting parameters from [Table 2, Table 2](#), and iii) by fitting the equations using the least-squares fitting algorithm. Using the first approach, we found that none of the equations could reasonably fit the experimental data when using an incorrect CEC and that each of the equations fit the experimental data reasonably well using the average parameters and the correct CEC ([Figure 3](#)), ([Fig. 2](#)). The relative goodness of average RSE under these conditions were 31% (Langmuir), 21% (Freundlich), 21% (Temkin), and 14% (Toth) (a full summary is given in [Table A3](#)). However, repeating this analysis using the average parameters from the separately fit equations ([Table A2](#)) results in an average RSE (for each ii) of 31% (Langmuir), 28% (Freundlich), 25% (Temkin), and 36% (Toth).

As was noted above, the Toth equation was the same only equation for the test set as for the training set, i.e. Toth>Temkin>Freundlich>Langmuir. We also tested an alternative approach for which the two approaches of calculating each equation’s fitting parameters, in which rather than average fitting parameters resulted in significantly different parameters. Most likely the fitting algorithm is over fitting the data due to the Toth equation having an additional parameter, making the Toth equation unreliable to generalize to uncharacterized soils. Additionally, while the Freundlich equation performs reasonably in this analysis using the pooled data fitting parameters, pooling the normalized data, and then fitting each curve, the curves were fit to each soil data from individual adsorption curve separately, and the resulting fitting parameters were then pooled. A full summary of the alternative fitting parameters and the test-set characterization is given in [Figure A1](#) and [Tables A21 – A43](#) curves created an implicit dependence of  $K_T$  on  $S_{max}$  (i.e. the saturation of adsorption at high concentrations), which is inconsistent with the behaviour of the Freundlich equation, which does not saturate at high concentrations. However, without a dependence on  $S_{max}$ , the Freundlich equation performs quite poorly at modelling uncharacterized soils. Consequently, we find that the Langmuir and Temkin equations are most suitable for use evaluating  $NH_4^+$  adsorption from uncharacterized soil samples.

Formatted: Indent: First line: 0.5"



220 **Figure 3:2:** Curve-fitting comparison between the unfitted Langmuir (red, solid), Freundlich (blue, ---), Temkin (green, - · - ·), and Toth (orange, · · ·) equations using the average-fitting parameters from Table 3 ~~the training set~~ applied to the test set of the a) Low CEC, b) Moderate CEC, c) High CEC samples (method ii)

Overall, we find that the Toth and Temkin equations best fit the full adsorption curves, while the Freundlich and Temkin equations best fit the low-range adsorption curves. However, both the Freundlich and Toth equations seem to be less robust when applied to this system than the Temkin equation. Firstly, the Freundlich equation, as formulated in Table 2 and Table 3, has an intrinsic dependence on the CEC, which is contrary to the theoretical basis of the Freundlich equation. Using the

225

Formatted: Normal

alternative fitting approach, the Freundlich equation does not require a CEC-dependence, but in that case, it has high error when fitting uncharacterized soils. Similarly, for the Toth equation, the alternative approach results in a significantly different set of fitting parameters, which resulted in the Toth equation quite poorly fitting the non-characterized soils. Additionally, while this may be a limitation of the fitting algorithm we selected, we found the Toth equation to be more difficult to consistently fit to our experimental data, with no solution being found for the low-range concentrations. Consequently, taking all of these factors into consideration, we find that the Temkin equation is most suitable for use evaluating  $\text{NH}_4^+$  adsorption from uncharacterized soil samples. For comparison with previous studies, in which the Langmuir equation is the most frequently used adsorption equation, we will continue to analyze it in subsequent sections, despite it performing much worse than the Temkin equation for both the low-range and full-range of data.

### 3.2. Determining aqueous $\text{NH}_4^+$ concentrations using the Langmuir and Temkin equations

To relate the total ammonium measured ( $m_{\text{NH}_4}$ ) to the adsorbed portion (S) and the aqueous portion (C), we define Eq.(7):

$$(7) m_{\text{NH}_4} = S + \frac{wC}{\rho}$$

Where  $m_{\text{NH}_4}$  is the total mass of ammonium per kg soil ( $\text{mg kg}^{-1}$ ),  $w$  the volumetric moisture content of the soil ( $\text{L water L}^{-1}$  soil), and  $\rho$  is the bulk density of the dry soil ( $\text{kg L}^{-1}$ ). By substituting the Langmuir (1) or Temkin (3) equations into Eq.(7),  $m_{\text{NH}_4}$  can be expressed in terms of C:

$$(8) m_{\text{NH}_4} = \frac{S_{\text{max}}K_L C}{1+K_L C} + \frac{wC}{\rho}$$

$$(9) m_{\text{NH}_4} = q_T \ln(1 + K_T C) + \frac{wC}{\rho}$$

To solve for C, we inverted these equations using *Wolfram Mathematica*, yielding Eq.(10) (Langmuir) and Eq.(11) (Temkin).

$$(10) C = \frac{-S_{\text{max}}K_L + K_L m_{\text{NH}_4} - Z + \sqrt{4K_L Z m_{\text{NH}_4} + (S_{\text{max}}K_L - K_L m_{\text{NH}_4} + Z)^2}}{2K_L Z}$$

$$(11) C = \frac{-Z + K_T q_T \cdot W\left(\frac{Z}{e^{K_T q_T} + \frac{m_{\text{NH}_4}}{q_T} \cdot Z}\right)}{K_T Z}, \text{ where } \mathbf{W}(\mathbf{x}) \text{ is the Lambert W function, and } Z = \frac{w}{\rho}$$

If it is assumed that  $m_{\text{NH}_4} \approx S$ , then  $\frac{wC}{\rho} \approx 0$ , and these equations can be simplified to Eq.(12) and Eq.(13) respectively.

$$(12) C = \frac{m_{\text{NH}_4}}{K_L(S_{\text{max}} - m_{\text{NH}_4})}$$

$$(13) C = \frac{e^{\frac{m_{\text{NH}_4}}{q_T}} - 1}{K_T}$$

We tested this assumption and found that for our unfertilized soil samples, the simplified equations have a positive bias of only 0.57 – 1.5%, and that for most soils fertilized with the equivalent of up to 300  $\text{kg N ha}^{-1}$ , the simplified equations should have a positive bias of less than 5%. Consequently, we used the simplified equations for our analysis.

### 3.3. Determining environmental soil emission potentials

255 Soil emission potentials were then calculated using the approaches described in Sect. 2.3.3, corresponding to the 'standard'  
 approach, two approaches based on matching the  $\text{NH}_4^+$  and pH extraction solutions, and two approaches based on applying  
 the Langmuir and Temkin equations to the measured extract concentrations and pH values. The adsorption equations were  
calculated using both the low-range and full curve fitting parameters. For the Langmuir calculations, the fit parameters were  
 $K_L = 9.29 \cdot 10^{-4} \text{ L kg}^{-1}$  (full) and  $K_L = 1.20 \cdot 10^{-3} \text{ L kg}^{-1}$  (low-range), and  $S_{\text{max}}$  calculated as the equivalent of the CEC in units of  
 260  $\text{mg kg}^{-1}$ . For the Temkin calculations, the fit parameters were  $K_T = 1.33 \cdot 10^{-2} \text{ L mg}^{-1}$ , and  $q_T (\text{mg kg}^{-1}) = 0.180 \cdot S_{\text{max}}$  (full) and  
 $K_T = 3.40 \cdot 10^{-2} \text{ L mg}^{-1}$ , and  $q_T (\text{mg kg}^{-1}) = 0.120 \cdot S_{\text{max}}$ . Among the approaches,  $\Gamma_{\text{STD}}$  results in the highest estimate for the  
 emission potential ( $17,000 \pm 19,000$ ), followed by  $\Gamma_{\text{Langmuir}}$  and  $\Gamma_{\text{SALT}}$  ( $2730 \pm 3530$ ), and  $\Gamma_{\text{Temkin}}$  and  $\Gamma_{\text{DIW}}$  ( $810 \pm 370 -$   
 1450) (Table 3). Emission potential is linearly related to equilibrium vapor pressure, at a temperature of  $15^\circ\text{C}$ , these  
 emission potentials correspond to equilibrium concentrations of  $2.4 - 50$  ppb. Although CEC is inversely related to the  
 265 proportion of  $\text{NH}_4^+$  present in the aqueous phase, the emission potentials increase exponentially as a function of the CEC due  
 to the strong positive correlation between soil pH and CEC (Figure 3).

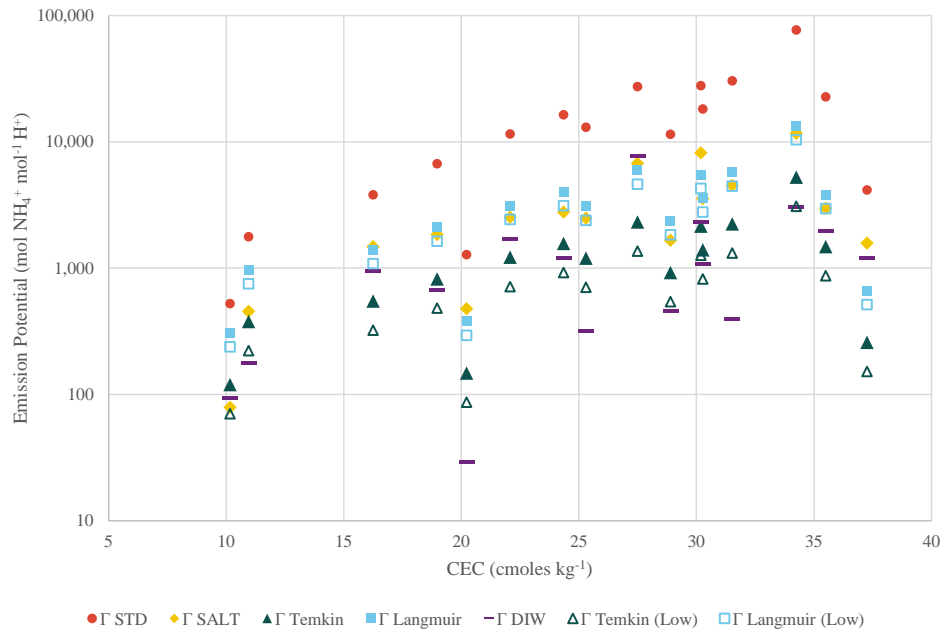
**Table 4:** Comparison of emission potentials determined using the standard, Langmuir, Temkin, salt extraction and DIW extraction methods.

Method	Equation	Average Emission Potential (mol mol <sup>-1</sup> ) (n = 16)	Equilibrium vapor pressure at 15°C (ppb)
$\Gamma_{\text{STD}}$	$\frac{[\text{NH}_4^+]_{\text{salt}}}{[\text{H}^+]_{\text{DIW}}}$	$17,000 \pm 19,000$	$50 \pm 55$
$\Gamma_{\text{SALT}}$	$\frac{[\text{NH}_4^+]_{\text{salt}}}{[\text{H}^+]_{\text{salt}}}$	$3300 \pm 3100$	$9.6 \pm 9.0$
$\Gamma_{\text{DIW}}$	$\frac{[\text{NH}_4^+]_{\text{DIW}}}{[\text{H}^+]_{\text{DIW}}}$	$1450 \pm 1900$	$4.2 \pm 5.5$
$\Gamma_{\text{Temkin (Full)}}$	$\frac{e^{\frac{[\text{NH}_4^+]_{\text{salt}}}{q_T} - 1}}{K_T} \frac{1}{[\text{H}^+]_{\text{DIW}}}$	$1370 \pm 1300$	$4.0 \pm 3.8$
$\Gamma_{\text{Temkin (Low-range)}}$		$810 \pm 740$	$2.4 \pm 2.2$
$\Gamma_{\text{Langmuir (Full)}}$ / $\Gamma_{\text{Temkin (Full)}}$	$\frac{[\text{NH}_4^+]_{\text{salt}}}{K_L(S_{\text{max}} - [\text{NH}_4^+]_{\text{salt}})} \frac{1}{[\text{H}^+]_{\text{DIW}}}$	$1370 - 1300 \pm 3530 \pm 3200$	$10 \pm 9.4 - 0 \pm 3.8$
$\Gamma_{\text{Langmuir (Low-Range)}}$	$\frac{e^{\frac{[\text{NH}_4^+]_{\text{salt}}}{q_T} - 1}}{K_L} \frac{1}{[\text{H}^+]_{\text{DIW}}}$	$3530 - 3200 \pm 2730 \pm 2500$	$7.7 \pm 7.10 \pm 9.3$

Merged Cells

Formatted Table

270



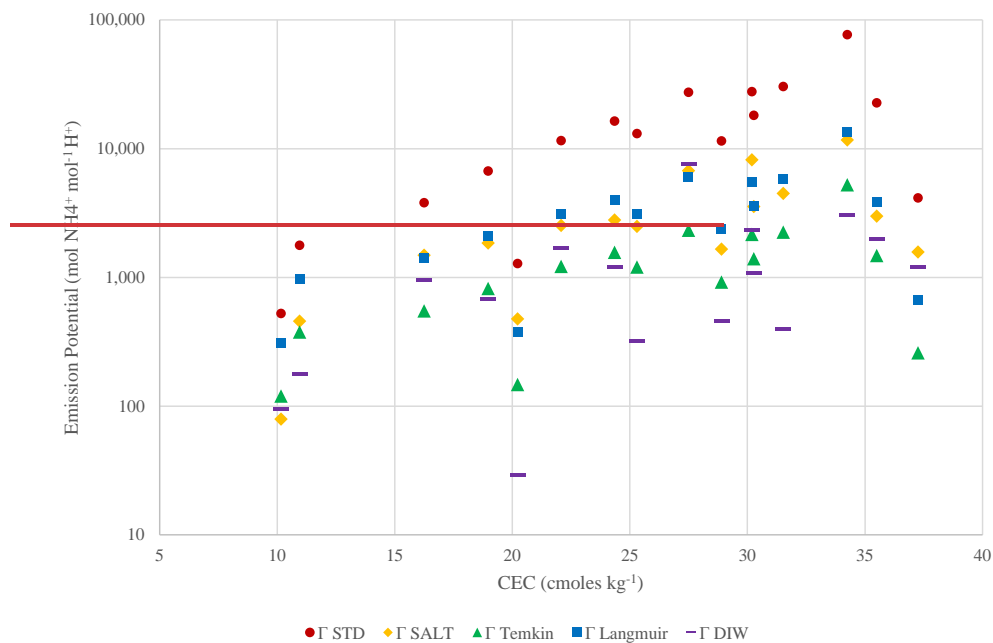


Figure 4.3: Soil emission potentials using the standard, salt extraction, Temkin, Langmuir and DIW extraction approaches, arranged by CEC.

275

#### 4. Discussion

The conventional approach for calculating emission potentials in soils lacks a solid theoretical foundation, and ought to be applied with caution. Empirically, this approach has performed poorly, with several studies reporting that calculated values of  $\Gamma_{STD}$  are unrealistically high and do not correspond well to measured or modelled emission fluxes (Cooter et al., 2010; Flechard et al., 2013; Neftel et al., 1998; Nemitz et al., 2001; Xu et al., 2022). Our assessment that the conventional method overestimates the soil emission potential by at least a factor of 5 is similar to findings reported by Nemitz et al., (2001) and Cooter et al., (2010) who reported needing to reduce their soil emission potentials by a factor of 6.66 and 2 – 3 respectively for their modelled predictions to match their flux observations. We believe that our empirical treatment of this system with the Langmuir and Temkin equations provides a more reasonable approach to estimate the soil emission potential. Additionally, in our view, the ‘like-with-like’ extraction approach (e.g.  $\Gamma_{SALT}$ -of  $\Gamma_{DIW}$ ) has a more ~~mechanistic~~ mechanistic and ~~theoretical~~ theoretical basis than the conventional

285



approach involving dissimilar extraction solutions. A few recent studies have reported on a similar approach using a Langmuir adsorption model (Alnsour, 2020; Guo et al., 2022b)2022), as well as by matching the  $\text{NH}_4^+$  and pH extraction solutions (Wu et al., 2023), showing that these methods can be feasibly implemented into an environmental sampling campaign. Venterea et al., (2015) reported that soil ammonium partitioning could be effectively modelled using a modified version of the Langmuir isotherm equation of the form  $S = \frac{S_{\max}C}{K+C}$ , where  $K$  ( $\text{mg L}^{-1}$ ) is the aqueous concentration at which  $S = \frac{1}{2} S_{\max}$ . The Venterea equation is equivalent to the Langmuir isotherm when  $K = \frac{1}{K_L}$ ; for the parameters determined in this study,  $\frac{1}{2}$  the saturation capacity is reached at exactly  $C = \frac{1}{K_L} = K$ , indicating that for our analysis the Langmuir and Venterea equations are equivalent.

How does this approach compare to the implementation of bidirectional exchange of  $\text{NH}_3$  in chemical transport models? Widely used models such as GEOS-CHEM and the EPA's CMAQ model soil emission potentials mechanistically, rather than being based on emission potentials prescribed using land-use categories (Bash et al., 2013; Pleim et al., 2013b)2013; Pleim, Ran, Appel, Shephard, et al., 2019; Zhu et al., 2015b)2015). In both models, the exchangeable soil ammonia has been parameterized as the volumetric molar concentration of ammonia in the top 1 – 5 cm divided by the volumetric water content in the soil, or  $[\text{NH}_4] = \frac{\text{NH}_4 \text{ mol m}^{-3}}{\theta \text{ m}^3 \text{ m}^{-3}}$  (Massad et al., 2010b)2010). In this parameterization, the entire soil ammonia content of the top layer of soil is treated as being dissolved into the soil water, thus a lower water content would result in a higher concentration of ammonia, and consequently a higher emission potential. (The parameter used by these models for the resistance to ammonia emissions from soil is inversely proportional to soil moisture, such that the actual emission of ammonia from soil would still be proportional to soil water content (Pleim et al., 2013b)2013.) In our model of the system, most ammonium is present adsorbed to soils, with the aqueous concentration controlled by the equilibrium between adsorbed and aqueous ammonium, increasing the soil water content would thus allow more ammonium to enter the aqueous phase to maintain the equilibrium concentration. (Increased water content could also result in nutrient runoff, reducing the soil ammonium content, or increased mineralization, increasing the soil ammonium content.) In the subsequent development of the bidirectional model coupled with an agricultural ecosystem model, Pleim et al., (2019) noted that reducing the ammonia available for emission by implementing the Langmuir adsorption isotherm approach proposed by Venterea et al. (2015) appeared to lead to unexpectedly low fractions of ammonia available for exchange. It may be that for recently fertilized soils, the applied fertilizer is not in contact with sufficient soil for this equilibrium relation to apply, and more research may be needed to understand the limitations and applications of both approaches. An updated version of CMAQ (v5.2.1) uses a Langmuir-derived approach described in Venterea et al. (2015) to predict  $\text{NH}_3$  bi-directional exchange and Kelly et al., (2019) explores its indirect impact on  $\text{PM}_{2.5}$  composition across the U.S., suggesting that the reduced emission potential from our approach is compatible with atmospheric agro-ecosystem modelling. -

Formatted: Subscript

315 **5. Conclusion**

This work evaluated the Langmuir, Freundlich, Temkin, and Toth adsorption isotherm equations as applied to environmental soil samples and  $\text{NH}_4^+$  partitioning. We determined that under ideal conditions the Toth equation was the most effective of these equations at fitting soil adsorption curves, but that the ~~Langmuir and Temkin equation was most~~ equations were more effective at predicting the adsorption behaviour of soil samples with minimal additional characterization required, and was  
320 effective over both low concentration ranges and when only the saturation concentration range, soil CEC was characterized. Applying this method to a series of environmental soil samples, we determined that the conventional method for directly measuring soil emission potentials may overestimate them by a factor of 5 – ~~20+2~~ (relative to using the Langmuir/Temkin equations respectively). Of the two adsorption equations, the Temkin equation fit the data better, with a significantly lower AIC (-222 vs -138 for the Langmuir equation). Comparing these empirical equations with an alternative approach for  
325 determining emission potential based on extracting  $\text{NH}_4^+$  and pH with the same extraction solutions (i.e. DIW/DIW or Salt/Salt) showed that the Temkin equation fit using the full adsorption range agreed well ~~equation-based approach is in good agreement~~ with the DIW/DIW equivalent-ratio based method, but was significantly different when using the low-range fitting parameters. ~~Of these four alternative methods, we suggest that the Temkin equation performs better at modelling the  $\text{NH}_4^+$  partitioning between soil and solution than the Langmuir equation.~~

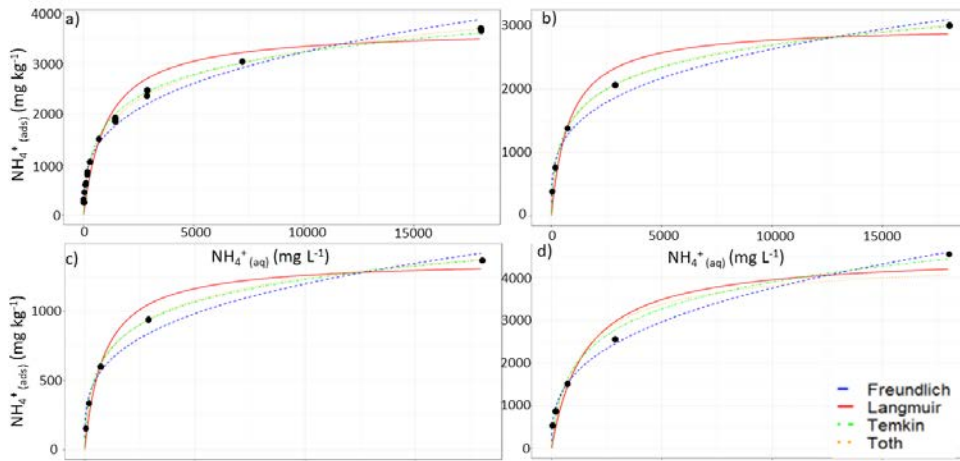


**Figure A1:** Curve-fitting comparison between the Langmuir (red, solid), Freundlich (blue, - - -), Temkin (green, · - · -), and Toth (orange, · · ·) equations for soil samples collected from a) King's College Circle, b) the University of Toronto Scarborough forest, c) High Park, and d) Queen's Park.

**Table A1:** Comparison of the residual standard errors, and the range of fitted parameters for adsorption curves fit to the un-pooled data. Parameters given in parentheses are reported for comparison with the parameters in Table 2. Goodness of fit is reported using the residual standard error (RSE) rather than AIC to avoid confusion between ranges of AICs for each equation.

Equation	Number of fitted parameters	RSE	Parameter 1	Mean ± sd	Parameter 2	Mean ± sd	Exponential Factor
Langmuir	1	17.5 – 25.7%	$K_L$	9.33E-4 ± 2.0E-4	-	-	-
Freundlich	2	5.72 – 17.6%	$K_F$	197 ± 60 ( $S_{max} * [0.053 ± 0.012]$ )	-	-	0.3064 ± 0.023
Temkin	2	3.0 – 16.1%	$K_T$	1.34E-2 ± 5.1E-3	$q_T$	$S_{max} * [0.183 ± 0.013]$	-
Toth	3	0.9 – 6.5%	$K_{To}$	3.75 ± 1.3	b	9960 ± 5590 ( $S_{max} * [2.42 ± 0.72]$ )	0.276 ± 0.054

**Table A2: Residual standard errors when applying average fit parameters from the pooled and (separately fit) training data to the test set soil samples, for i) a CEC of 25; ii) the experimentally measured CEC; iii) when the data is fit using the fitting algorithm**

Sample Location	CEC (cmole kg <sup>-1</sup> )	NH <sub>4</sub> <sup>+</sup> (mg kg <sup>-1</sup> )	pH	RSE (%) using estimated fit parameters				
				Langmuir	Freundlich	Temkin	Toth	
High Park	10.95	2.906	7.04	280 (285)	330 (340)	320 (330)	330 (420)	
				26 (26)	22 (26)	16 (18)	14 (28)	
				25	19	14	8.8	
Corktown	25.3	3.552	7.82	33 (33)	25 (31)	22 (26)	9.5 (39)	
				34 (34)	28 (34)	25 (28)	9.7 (43)	
				29	15	15	3.8	
Riverdale Park East	37.25	2.835	7.42	64 (63)	62 (58)	66 (63)	84 (62)	
				35 (35)	19 (25)	29 (31)	19 (39)	
				31	11	24	23	
Geometric Mean RSE		Estimated		84 (84)	80 (85)	77 (81)	64 (100)	
				Estimated with measured CEC	31 (31)	21 (28)	21 (25)	14 (36)
				Fitted Equation	28.3	14.8	17.0	9.2

**Table A3: Sample information for the adsorption test set**

Sample	CEC (cmole kg <sup>-1</sup> )	Bulk NH <sub>4</sub> <sup>+</sup> (mg kg <sup>-1</sup> )	pH	Extractant Solution (mg L <sup>-1</sup> )	Soil Mass (g)	Sum of displaced cations (cmole kg <sup>-1</sup> )	NH <sub>4</sub> <sup>+</sup> adsorbed (mg kg <sup>-1</sup> )
High Park	10.95	2.906	7.04	18.04	1.006	0.989	178.4
				36.08	1.0124	0.949	171.2
				144.32	0.9953	1.951	351.9
				721.6	0.9976	4.028	726.6
				3608	0.9539	7.413	1337
				18040	1.0002	10.81	1950
Corktown	25.3	3.552	7.82	18.04	1.0081	1.793	323.5
				36.08	1.0095	2.222	400.9
				144.32	0.9944	4.228	762.8
				721.6	1.0013	9.064	1635
				3608	1.0131	15.54	2804

				<u>18040</u>	<u>1.002</u>	<u>24.39</u>	<u>4400</u>
<u>Riverdale Park East</u>	<u>37.25</u>	<u>2.835</u>	<u>7.42</u>	<u>18.04</u>	<u>0.9948</u>	<u>4.447</u>	<u>802.2</u>
				<u>36.08</u>	<u>1.0193</u>	<u>4.861</u>	<u>876.8</u>
				<u>144.32</u>	<u>1.0151</u>	<u>6.690</u>	<u>1207</u>
				<u>721.6</u>	<u>1.0304</u>	<u>11.79</u>	<u>2127</u>
				<u>3608</u>	<u>0.9953</u>	<u>23.53</u>	<u>4244</u>
				<u>18040</u>	<u>1.027</u>	<u>36.26</u>	<u>6541</u>

### 345 **Author contribution statement**

MGD: Investigation, Formal analysis, Writing – Original Draft; KY: Investigation, Methodology; JGM: Supervision, Funding acquisition, Writing – Review & Editing.

### **Competing interests statement**

The authors declare that they have no conflict of interest.

### 350 **Funding statement**

This research was supported by a Natural Science and Engineering Research Council (NSERC) Discovery grant and a Grants and Contributions agreement GCXE19S016 with Environment and Climate Change Canada held by Jennifer Murphy. Matthew Davis held a Walter C. Sumner Memorial Fellowship while conducting this research. An Undergraduate Summer Research Award from NSERC supported Kevin Yan during this work.

### 355 **Acknowledgements**

We thank our colleagues Professor Myrna Simpson and Jenny Oh (University of Toronto) for their helpful discussions. We also thank the University of Toronto ANALEST facility staff for their technical assistance.

## References

- Alnsour, N. I. (2020). *Bi-Directional Exchange of Ammonia from Soils in Row Crop Agro-ecosystems*. North Carolina State University.
- 360 Bache, B. W. (1976). The measurement of cation exchange capacity of soils. *Journal of the Science of Food and Agriculture*, 27(3), 273–280. <https://doi.org/10.1002/jsfa.2740270313>
- Bash, J. O., Cooter, E. J., Dennis, R. L., Walker, J. T., & Pleim, J. E. (2013). Evaluation of a regional air-quality model with bidirectional NH<sub>3</sub> exchange coupled to an agroecosystem model. *Biogeosciences*, 10(3), 1635–1645.
- 365 <https://doi.org/10.5194/bg-10-1635-2013>
- Bouwman, A. F., Lee, D. S., Asman, W. A. H., Dentener, F. J., Hoek, K. W. Van Der, Olivier, J. G. J., Tg, N., & Tg, N. (1997). A global high-resolution emission inventory for ammonia. *Global Biogeochemical Cycles*, 11(4), 561–587.
- Chu, K. H. (2021). Revisiting the Temkin Isotherm: Dimensional Inconsistency and Approximate Forms. *Industrial and Engineering Chemistry Research*, 60(35), 13140–13147. <https://doi.org/10.1021/acs.iecr.1c01788>
- 370 Cooter, E. J., Bash, J. O., Walker, J. T., Jones, M. R., & Robarge, W. (2010). Estimation of NH<sub>3</sub> bi-directional flux from managed agricultural soils. *Atmospheric Environment*, 44(17), 2107–2115. <https://doi.org/10.1016/j.atmosenv.2010.02.044>
- Ellis, E. C., Beusen, A. H. W., & Goldewijk, K. K. (2020). Anthropogenic biomes: 10,000 BCE to 2015 CE. *Land*, 9(5), 8–10. <https://doi.org/10.3390/LAND9050129>
- 375 Farquhar, G. D., Firth, P. M., Wetselaar, R., & Weir, B. (1980). On the Gaseous Exchange of Ammonia between Leaves and the Environment: Determination of the Ammonia Compensation Point. *Plant Physiology*, 66(4), 710–714. <https://doi.org/10.1104/pp.66.4.710>
- Flechard, C. R., Fowler, D., Sutton, M. A., & Cape, J. N. (1999). A dynamic chemical model of bi-directional ammonia exchange between semi-natural vegetation and the atmosphere. In *Quarterly Journal of the Royal Meteorological Society* (Vol. 125, Issue 559). <https://doi.org/10.1002/qj.49712555914>
- 380 Flechard, C. R., Massad, R.-S., Loubet, B., Personne, E., Simpson, D., Bash, J. O., Cooter, E. J., Nemitz, E., & Sutton, M. A. (2013). Advances in understanding, models and parameterizations of biosphere-atmosphere ammonia exchange. *Biogeosciences*, 10(7), 5183–5225. <https://doi.org/10.5194/bg-10-5183-2013>
- 385 Freundlich, H. (1909). *Kapillarchemie: eine Darstellung der Chemie der Kolloide und verwandter Gebiete*. In *Akademische Verlagsgesellschaft*. Verlag der Akademischen Verlagsgesellschaft. <https://doi.org/10.1038/130866a0>
- 390 Guo, X., Pan, D., Daly, R. W., Chen, X., Walker, J. T., Tao, L., McSpurr, J., & Zondlo, M. A. (2022a). [Spatial heterogeneity of ammonia fluxes in a deciduous forest and adjacent grassland. \*Agricultural and Forest Meteorology\*, 326\(July\), 109128. https://doi.org/10.1016/j.agrformet.2022.109128](https://doi.org/10.1016/j.agrformet.2022.109128)

- Guo, X., Pan, D., Daly, R. W., Chen, X., Walker, J. T., Tao, L., McSparrill, J., & Zondlo, M. A. (2022b). Spatial heterogeneity of ammonia fluxes in a deciduous forest and adjacent grassland. *Agricultural and Forest Meteorology*, 326(July), 109128. <https://doi.org/10.1016/j.agrformet.2022.109128>
- 395 Kelly, J. T., Kopplitz, S. N., Baker, K. R., Holder, A. L., Pye, H. O. T., Murphy, B. N., Bash, J. O., Henderson, B. H., Possiel, N. C., Simon, H., Eyth, A. M., Jang, C., Phillips, S., & Timin, B. (2019). Assessing PM2.5 model performance for the conterminous U.S. with comparison to model performance statistics from 2007-2015. *Atmospheric Environment*, 214(May), 116872. <https://doi.org/10.1016/j.atmosenv.2019.116872>
- Kempers, A. J., & Zweers, A. (1986). Ammonium determination in soil extracts by the salicylate method. *Communications in Soil Science and Plant Analysis*, 17(7), 715–723. <https://doi.org/10.1080/00103628609367745>
- 400 Langmuir, I. (1916). The Constitution and Fundamental Properties of Solids and Liquids. Part I. Solids. *Journal of the American Chemical Society*, 38(11), 2221–2295.
- Li, K. yi, Zhao, Y. yuan, Yuan, X. long, Zhao, H. bing, Wang, Z. hui, Li, S. xiu, & Malhi, S. S. (2012). Comparison of Factors Affecting Soil Nitrate Nitrogen and Ammonium Nitrogen Extraction. *Communications in Soil Science and Plant Analysis*, 43(3), 571–588. <https://doi.org/10.1080/00103624.2012.639108>
- 405 Massad, R. S., Nemitz, E., & Sutton, M. A. (2010a). [Review and parameterisation of bi-directional ammonia exchange between vegetation and the atmosphere. \*Atmospheric Chemistry and Physics\*, 10\(21\), 10359–10386. https://doi.org/10.5194/acp-10-10359-2010](https://doi.org/10.5194/acp-10-10359-2010)
- 410 [Massad, R. S., Nemitz, E., & Sutton, M. A. \(2010b\). Review and parameterisation of bi-directional ammonia exchange between vegetation and the atmosphere. \*Atmospheric Chemistry and Physics\*, 10\(21\), 10359–10386. https://doi.org/10.5194/acp-10-10359-2010](https://doi.org/10.5194/acp-10-10359-2010)
- Neftel, A., Blatter, A., Gut, A., Högger, D., Meixner, F., Ammann, C., & Nathaus, F. J. (1998). NH<sub>3</sub> soil and soil surface gas measurements in a triticale wheat field. *Atmospheric Environment*, 32(3), 499–505. [https://doi.org/10.1016/S1352-2310\(97\)00162-3](https://doi.org/10.1016/S1352-2310(97)00162-3)
- 415 Nemitz, E., Milford, C., & Sutton, M. A. (2001). A two layer canopy compensation point model for describing bi-directional biosphere-atmosphere exchange of ammonia. *Q. J. R. Meteorol. Soc.*, 127, 815–833.
- Nemitz, E., Sutton, M. A., Schjoerring, J. K., Husted, S., & Paul Wyers, G. (2000). Resistance modelling of ammonia exchange over oilseed rape. *Agricultural and Forest Meteorology*, 105(4), 405–425. [https://doi.org/10.1016/S0168-1923\(00\)00206-9](https://doi.org/10.1016/S0168-1923(00)00206-9)
- 420 Pleim, J. E., Bash, J. O., Walker, J. T., & Cooter, E. J. (2013a). [Development and evaluation of an ammonia bidirectional flux parameterization for air quality models. \*Journal of Geophysical Research: Atmospheres\*, 118\(9\), 3794–3806. https://doi.org/10.1002/jgrd.50262](https://doi.org/10.1002/jgrd.50262)
- [Pleim, J. E., Bash, J. O., Walker, J. T., & Cooter, E. J. \(2013b\).2013. Development and evaluation of an ammonia bidirectional flux parameterization for air quality models. \*Journal of Geophysical Research: Atmospheres\*, 118\(9\), 3794–3806. https://doi.org/10.1002/jgrd.50262](https://doi.org/10.1002/jgrd.50262)

- 425 Pleim, J. E., Ran, L., Appel, W., & Shephard, M. W. (2019). *New Bidirectional Ammonia Flux Model in an Air Quality Model Coupled With an Agricultural Model*. *Journal of Advances in Modeling Earth Systems*, 2934–2957. <https://doi.org/10.1029/2019MS001728>
- Pleim, J. E., Ran, L., Appel, W., Shephard, M. W., & Cady-Pereira, K. (2019). New Bidirectional Ammonia Flux Model in an Air Quality Model Coupled With an Agricultural Model. *Journal of Advances in Modeling Earth Systems*, 11(9), 2934–2957. <https://doi.org/10.1029/2019MS001728>
- 430 Spiess, A. N., & Neumeyer, N. (2010). An evaluation of R2 as an inadequate measure for nonlinear models in pharmacological and biochemical research: A Monte Carlo approach. *BMC Pharmacology*, 10, 1–11. <https://doi.org/10.1186/1471-2210-10-6>
- Sutton, M. A., Erismann, J. W., Dentener, F., & Möller, D. (2008). Ammonia in the environment: From ancient times to the present. *Environmental Pollution*, 156(3), 583–604. <https://doi.org/10.1016/j.envpol.2008.03.013>
- 435 Sutton, M. A., Reis, S., Riddick, S. N., Dragosits, U., Nemitz, E., Theobald, M. R., Tang, Y. S., Braban, C. F., Veno, M., Dore, A. J., Mitchell, R. F., Wanless, S., Daunt, F., Fowler, D., Blackall, T. D., Milford, C., Flechard, C. R., Loubet, B., Massad, R., ... de Vries, W. (2013). Towards a climate-dependent paradigm of ammonia emission and deposition. *Philosophical Transactions of the Royal Society B: Biological Sciences*, 368(1621). <https://doi.org/10.1098/rstb.2013.0166>
- 440 Sutton, M. A., Schjørring, J. K., & Wyers, G. P. (1995). Plant-atmosphere exchange of ammonia. *Philos. T. R. Soc. Lond., A*, 351(29), 261–276.
- Temkin, M. I., & Pyzhev, V. (1940). Kinetics of ammonia synthesis on promoted iron catalyst. *Acta Phys. Chim. USSR*, 12(327).
- 445 Tóth, J. (1995). Uniform interpretation of gas/solid adsorption. *Advances in Colloid and Interface Science*, 55(C), 1–239. [https://doi.org/10.1016/0001-8686\(94\)00226-3](https://doi.org/10.1016/0001-8686(94)00226-3)
- Van Aardenne, J. A., Dentener, F. J., Olivier, J. G. J., Goldewijk, C. G. M. K., & Lelieveld, J. (2001). A 1° × 1° resolution data set of historical anthropogenic trace gas emissions for the period 1890–1990. *Global Biogeochemical Cycles*, 15(4), 909–928. <https://doi.org/10.1029/2000GB001265>
- 450 Venterea, R. T., Clough, T. J., Coulter, J. A., & Breuillin-Sessoms, F. (2015). Ammonium sorption and ammonia inhibition of nitrite-oxidizing bacteria explain contrasting soil N2O production. *Scientific Reports*, 5(April), 1–15. <https://doi.org/10.1038/srep12153>
- Vogeler, I., Cichota, R., Snow, V. O., Dutton, T., & Daly, B. (2011). Pedotransfer Functions for Estimating Ammonium Adsorption in Soils. *Soil Science Society of America Journal*, 75(1), 324–331. <https://doi.org/10.2136/sssaj2010.0192>
- 455 [Walker, J. T., Chen, X., Wu, Z., Schwede, D., Daly, R., Djurkovic, A., Oishi, A. C., Edgerton, E., Bash, J., Knoepp, J., Puchalski, M., Iames, J., & Miniati, C. F. \(2023\). Atmospheric deposition of reactive nitrogen to a deciduous forest in the southern Appalachian Mountains. \*Biogeosciences\*, 20\(5\), 971–995. <https://doi.org/10.5194/bg-20-971-2023>](#)



460 Wentworth, G. R., Murphy, J. G., Gregoire, P. K., Cheyne, C. A. L., Tevlin, A. G., & Hems, R. (2014). Soil-atmosphere  
exchange of ammonia in a non-fertilized grassland: Measured emission potentials and inferred fluxes. *Biogeosciences*,  
11(20), 5675–5686. <https://doi.org/10.5194/bg-11-5675-2014>

Wu, Z., Walker, J. T., Oishi, A. C., Duman, T., Katul, G., Chen, X., Schwede, D., Bash, J., & Iiames, J. (2023).  
Estimating source-sink distributions and fluxes of reactive nitrogen and sulfur within a mixed forest canopy.  
*Agricultural and Forest Meteorology*, 333(June 2022), 109386. <https://doi.org/10.1016/j.agrformet.2023.109386>

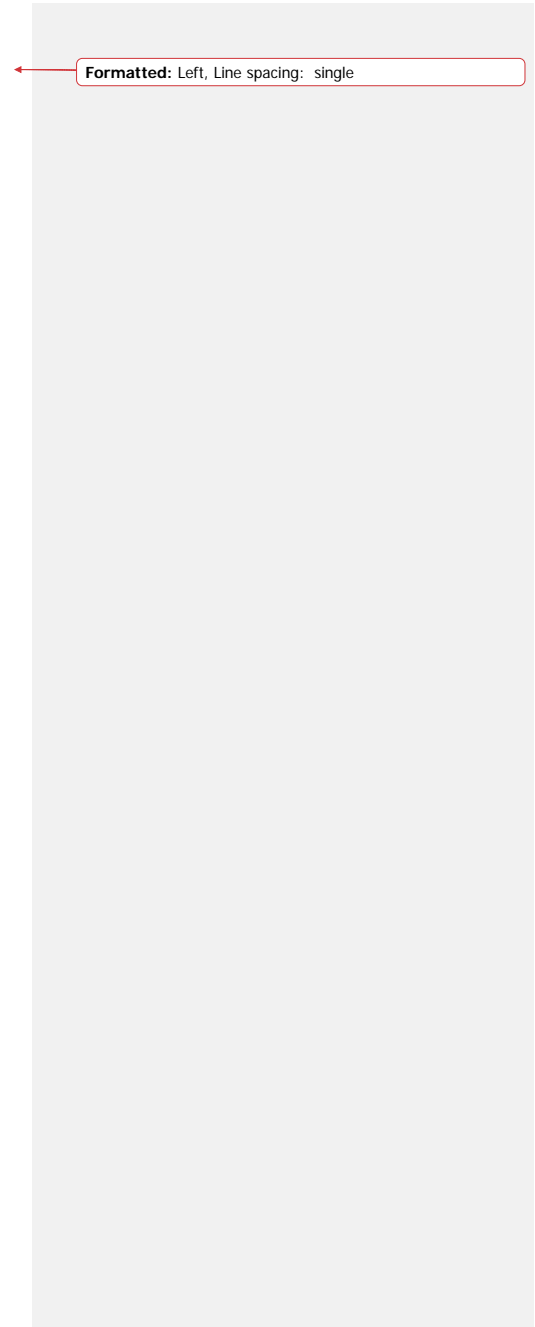
465 Xu, M., Umehara, M., Sase, H., & Matsuda, K. (2022). Ammonia fluxes over an agricultural field in growing and fallow  
periods using relaxed eddy accumulation. *Atmospheric Environment*, 284(April), 119195.  
<https://doi.org/10.1016/j.atmosenv.2022.119195>

Zhang, L., Wright, L. P., & Asman, W. A. H. (2010). Bi-directional air-surface exchange of atmospheric ammonia: A review  
of measurements and a development of a big-leaf model for applications in regional-scale air-quality models. *Journal of  
470 Geophysical Research Atmospheres*, 115(20). <https://doi.org/10.1029/2009JD013589>

Zhu, L., Henze, D., Bash, J., Jeong, G. R., Cady-Pereira, K., Shephard, M., Luo, M., Paulot, F., & Capps, S. (2015a). Global  
evaluation of ammonia bidirectional exchange and livestock diurnal variation schemes. *Atmospheric Chemistry and  
Physics*, 15(22), 12823–12843. <https://doi.org/10.5194/acp-15-12823-2015>

Zhu, L., Henze, D., Bash, J., Jeong, G. R., Cady-Pereira, K., Shephard, M., Luo, M., Paulot, F., & Capps, S. (2015b).).  
475 Global evaluation of ammonia bidirectional exchange and livestock diurnal variation schemes. *Atmospheric  
Chemistry and Physics*, 15(22), 12823–12843. <https://doi.org/10.5194/acp-15-12823-2015>

|



Formatted: Left, Line spacing: single